Acoustic response of thin-walled, orthogonally stiffened cylinders

IOP Conf. Series: Materials Science and Engineering **657** (2019) 012007 doi:10.1088/1757-899X/657/1/012007

Acoustic response of thin-walled, orthogonally stiffened cylinders

D Zhao[1,2], N S Ferguson[1] and G Squicciarini[1]

[1]Institute of Sound and Vibration, University of Southampton, UK

E-mail: Dong.Zhao@soton.ac.uk

Abstract. A semi-analytical model is developed to predict the acoustic response of thin-walled, orthogonally stiffened cylinders. The free vibration model is solved by the approximate assumed-modes method. The excitation of the normal modes is considered in terms of the Joint Acceptance Function (JAF) for incident acoustic harmonic plane waves. The surface pressure distribution is obtained by the shallow shell approximation, where the blocked excitation pressure is double the incident pressure, and by the 2-D rigid cylinder approximation considering the sound scattering. The acoustic response is then compared with that of a fully coupled FE-BE model. An efficient estimation of the response can be obtained by the two models over a certain range of accuracy. Numerical results for different structural configurations are then given. The effect of the stiffeners on the modal characteristics is discussed. It also illustrates the modal contribution to the total displacement response and addresses both circumferential and axial orthogonally stiffened cylinder arrangements.

1. Introduction

Thin-walled, stiffened cylinders are representative of widely used aerospace structures. When subjected to high-level acoustic loading, typically from rocket or jet engines, such structures are likely to experience considerable vibration and stress reversals, which may lead to fatigue failure. An efficient and accurate prediction of acoustically induced vibration (AIV) is thus required.

Much progress has been made in the past to predict the dynamic response of stiffened structures subjected to sound pressure. Often, flat structures are considered, and this significantly simplifies the structural modelling and acoustic response prediction [1-3]. The acoustically excited modes can be characterized by a structure-acoustic coupling ratio, the Joint Acceptance Function (JAF), which effectively relates the modal forces to the spatial matching between the acoustic field and the structural mode [4]. The acoustic response of stiffened plates has been analysed in a recent study by the authors [5]. However, these assumptions are not necessary applicable for curved structures. In comparison to stiffened flat plates, the stiffeners produce different effects on the modal characteristics of the cylinders due to the coupling of extension/bending motion around the circumference [6,7]. In addition, scattering effects must be considered for cylinders; for flat structures modelling of the excitation assumes that the blocked pressure is the twice that of the incident pressure and it is even appropriate for panels with small curvatures [8], but this assumption is invalid for a structure with significant curvature, whose dimension is comparable to the acoustic wavelength [9]. The JAFs of diffuse field has been investigated for cylindrical geometries based on a suitable spatial correlation function [10]. To the best of authors' knowledge, the acoustic scattering has not been explicitly addressed in the AIV within the aerospace domain. An exact solution for this problem requires a fully

coupled vibroacoustic analysis, usually provided using a model that combines the structural model (FEM) and the acoustic domain (BEM). However, this approach requires high computational resources and it is not always practical for preliminary investigation and parametric study. Alternatively, the vibroacoustic response can be predicted by developing pre-processing tools compatible with commercial FE codes to reduce the computational cost. In this sense, Seon and Roy [11] developed a pre-processing tool to perform vibroacoustic analysis in Nastran for the Thermal Protection Panels (TPS) in a launch vehicle. For more generalized structures, like stiffened cylinders, an efficient model incorporating features like stiffener configurations and scattering is necessary for the preliminary studies.

This paper presents a semi-analytical approach to predict the linear response of stiffened cylinders to harmonic plane wave excitation. The free vibration problem is formulated by the assumed-modes method. The subsequent modal forces are derived based on two approximations for the pressure distribution: (i) blocked pressure around the cylinder and (ii) 2-D scattered pressure. These approaches are then compared with the results of a fully coupled vibroacoustic analysis from a FE/BE model.

2. The free vibration

The formulation adopted in this work to express the energy of the vibrating stiffened cylinder follows the procedures in reference [6]. Figure 1 shows the geometry of a thin-walled cylinder which is internally stiffened by a set of rings (around the circumference) and by a set of stringers (along the length). The flexure and extension of the cylindrical shell are considered. As a result of these deformations, the stiffeners are subjected to flexure (about two perpendicular axes), extension and torsion. From the linear strain-displacement relation [12] and the equation of state for the plane stress, the strain energy for the cylinder and the stiffeners can be formulated as a function of the displacement. The displacement of the stiffeners is uncoupled using the elastic axis and referenced to that of the line of attachment. Then, the compatibility conditions between the cylinder and the stiffeners are adopted to express the total energy in terms of the displacement of the cylinder middle surface. The detailed derivation can be found in reference [6]. The end boundary conditions of the cylinder are assumed to be shear diaphragms (S-D) [13]. The displacement of the middle surface of the cylinder can be expressed as,

$$
\begin{aligned}
u &= \sqrt{2}\sum_m\sum_n (\bar{u}_{mn}\cos n\theta + \bar{u}'_{mn}\sin n\theta)\cos m\pi x/a \\
v &= \sqrt{2}\sum_m\sum_n (\bar{v}_{mn}\sin n\theta - \bar{v}'_{mn}\cos n\theta)\sin m\pi x/a \\
w &= \sqrt{2}\sum_m\sum_n (\bar{w}_{mn}\cos n\theta + \bar{w}'_{mn}\sin n\theta)\sin m\pi x/a
\end{aligned}
\tag{1}
$$

where $\bar{u}_{mn}$, $\bar{v}_{mn}$ and $\bar{w}_{mn}$ are the generalized coordinates of the symmetric circumferential modes and $\bar{u}'_{mn}$, $\bar{v}'_{mn}$ and $\bar{w}'_{mn}$ are those of the antisymmetric modes.

The homogeneous equations of motion have been obtained by substituting the energy expression and equation (1) into Lagrange's equation [14]. The resulting frequency equation have been numerically solved in MATLAB to obtain the natural frequencies and mode shapes of the stiffened cylinder.

3. The acoustic response

Figure 2 shows that an acoustic harmonic plane wave impinging on the outer surface of a cylinder with an incident angle β to the x axis. Without losing any generality, it is convenient to assume that the incident acoustic wave component in the $y-z$ plane only travels along the y axis. In this paper it is assumed that the two closed ends of the cylinder have no influence to the acoustic field, i.e., the

diffraction and scattering due to the finite length of cylinder are neglected. To simplify the analysis, the 3-D incident plane wave is written in cylindrical coordinates as,

$$p_i(\theta, s, t) = p_0 \sum_{q=-\infty}^{\infty} (-i)^q J_q(kR\cos(\beta))\mathrm{e}^{iq\theta}\mathrm{e}^{ikRs\sin\beta}\mathrm{e}^{i\omega t}, \tag{2}$$

where J_q is the Bessel function of first kind of order q and ϵ_q is the Neumann factor. p_0 is the amplitude of the free field incident pressure and $s = x/R$ is a normalized coordinate.

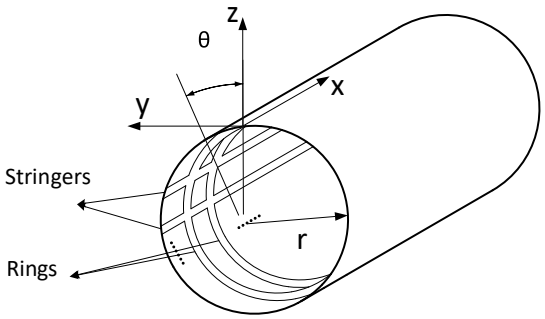

Figure 1. Geometry of a stiffened cylinder with the coordinate system.

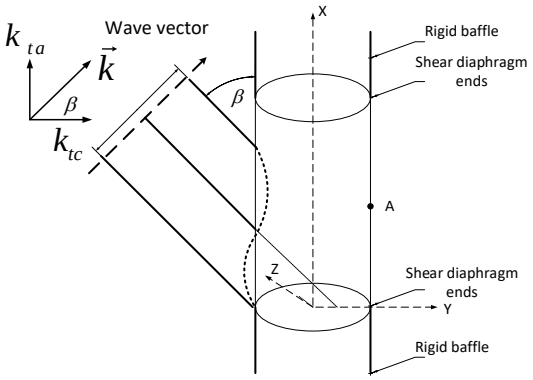

Figure 2. Diagram of an incident plane wave. k is the acoustic wavenumber and k_{ta}, k_{tc} are respectively the acoustic trace wavenumber (projection) along and normal to the shell axis.

3.1. Joint acceptance function (JAF) for the shallow shell assumption

In the blocked pressure assumption, the total pressure distribution can be represented as

$$p(\theta, s, t) = 2p_i(\theta, s, t). \tag{3}$$

Note that this is only a rough approximation that maybe valid only for some points of the cylinder and in a frequency range where the acoustic wavelength is small compared to the radius of curvature of the cylinder. From the modal analysis [14], the modal forces are,

$$L_{mn}(t) = \int_0^{2\pi}\int_0^{l/R} p(\theta, s, t)\phi_{mn}(\theta, s)\mathrm{d}sR\mathrm{d}\theta = F_0 j_{mn}(\omega)\mathrm{e}^{i\omega t} \tag{4}$$

where $F_0 = p_0 S$ is defined as an equivalent static force acting on the cylinder surface with a normalized area $S = 2R\sqrt{\pi R l}$. The area has been normalized to simplify the expression for the JAF. $j_{mn}(\omega) = j_{Rn}(k_{tr}R)j_{Am}(k_{ta}l)$ can be regarded as the JAF for the $(m,n)^{th}$ mode of the cylinder for this type of incident pressure field. j_{Rn} and j_{Am} are therefore its circumferential and axial components respectively. They are given by the expressions

$$j_{Cn}(k_{tc}R) = (-i)^n J_n(k_{tc}R) \tag{5}$$

$$j_{Am}(k_{ta}l) = \frac{(-1)^m e^{-ik_{ta}l} - 1}{(k_{ta}l)^2 - (m\pi)^2} m\pi, \tag{6}$$

where k_{tc} and k_{ta} are the trace wavenumbers in the circumferential and axial directions, namely

$$k_{tc} = k\cos\beta\,,\; k_{ta} = k\sin\beta.$$

3.2. JAF using a 2-D rigid cylinder assumption for the scattered pressure

When the radius of the cylinder is comparable to the acoustic wavelength, the sound scattering due to the curvature will be significant. Assuming a rigid cylinder, the total pressure is in this case [15]:

$$p_t(\theta, s, t) = p_0 \sum_{q=-\infty}^{\infty} (-i)^q \left(J_q(k_{tc}R) - R_q(k_{tc}R)\right) \mathrm{e}^{iq\theta} \mathrm{e}^{ik_{ta}Rs} \mathrm{e}^{i\omega t}. \tag{7}$$

$$where\ R_q(k_{tc}R) = \left(\frac{J_{q-1}(k_{tc}R) - J_{q+1}(k_{tc}R)}{H^{(2)}_{q-1}(k_{tc}R) - H^{(2)}_{q+1}(k_{tc}R)}\right) H^{(2)}_q(k_{tc}R). \tag{8}$$

$H^{(2)}_n(kR)$ are Hankel functions of the second kind.

It can be seen that only the pressure distribution in the circumferential direction is influenced by the scattering effect. The axial JAF remains the same to equation (6). The circumferential JAF becomes

$$j^t_{Cn}(k_{tc}R) = (-1)^n [J_n(k_{tc}R) - R_n(k_{tc}R)]. \tag{9}$$

4. Numerical results and discussion

Four types of structural configurations are considered for the aluminium cylinders. They are a bare cylinder, a cylinder stiffened by 9 equally spaced rings, a cylinder stiffened by 8 equally spaced stringers and a cylinder stiffened by both rings and stringers of the same number and positions. The dimensions and the material properties are given in table 1. Stringers and rings have rectangular cross section. In the numerical calculation, hysteric damping is assumed by using a damping loss factor of 1%. The numerical simulation is performed in the MATLAB.

Table 1. Parameters for numerical simulation of an aluminium cylinder.

Parameters	Symbol	Value	Parameters	Symbol	Value
Cylinder radius (m)	r	0.9	ring width (m)	r_w	0.002
Cylinder length (m)	l	0.3	ring depth (m)	r_d	0.004
Cylinder thickness (m)	t	0.002	Stringer width (m)	s_w	0.002
Density (kg/m^3)	ρ	2.7×10^3	Stringer depth (m)	s_d	0.004
Poisson's ratio	ν	0.3	Elastic modulus (N/m^2)	E	71×10^9
Incident angle (rad)	β	$\pi/4$	Pressure amplitude (Pa)	p_0	1

Figure 3 gives the natural frequencies of the lowest 20 modes for each structural configurations denoted by different types of symbols. The natural frequencies of adjacent modes appear in pairs for each structural configuration. This is because all the cylinders are symmetric. Each pair of frequencies corresponds to the symmetric/anti-symmetric modes. They are equal for the bare cylinder and slightly different for the stiffened ones. Compared to the bare cylinder, the rings increase the natural frequencies in each mode while the stringers decrease them slightly. This is because these modes are dominated by the circumferential deformation. The rings constrain the extensional or the flexural motions for these modes, which effectively stiffens the cylinder. The stringers put no constraint but apply mass to these modes. The natural frequencies of ring-stiffened cylinders also tend to occur in clusters over a small frequency range. This is because the stiffness effect of the rings makes the cylinder more like a finite periodic structure characterized by the 'frequency passband'.

Figure 4 plots the absolute values of the circumferential and the axial JAFs against the non-dimensional parameters, $k_{tc}R$ and $k_{ta}l$. These are for the bare cylinder and are based on the blocked pressure approximation. The results show a series of maxima for each mode. The maximum value occurs in the mode with the lowest order, corresponding to the 'breathing' mode for the circumferential direction and to the 'beam' bending mode in the axial direction. However, these modes occur at relatively high frequency for this geometry, being at 907 Hz (breathing mode) and 897 Hz

(beam bending mode) and corresponding to mode number 135 and 131. For the other modes, the maxima in the axial JAF occur when the acoustic trace wavenumber matches the structural bending wavenumber, which is known as coincidence phenomenon. The maxima of the circumferential JAF results from the combination of pressure distribution around the circumference and the mode shapes. The pressure distribution around the circumference due to the incident plane waves does not result in a constant acoustic wavelength. It is therefore not straightforward to associate maxima in the circumferential JAF to the same coincidence phenomena found in the axial direction (or in flat plates). The dips in the JAFs correspond to the zero modal force, which occur when the integrations of the production of pressure and mode shape on the cylinder surface equal to zero in equation (4).

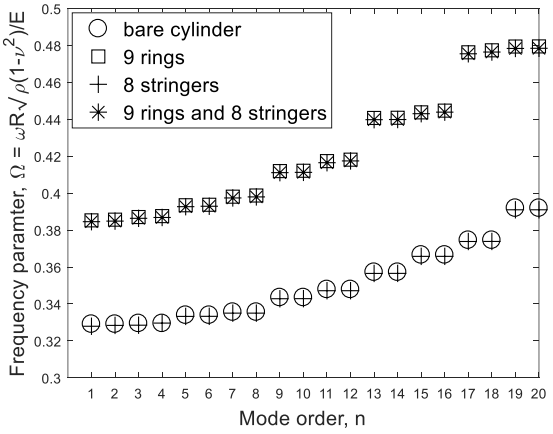

Figure 3. The natural frequencies of the lowest 20 modes for each case, plotted versus non-dimensional frequency $\Omega = \omega/\omega_R$ where $\omega_R = \sqrt{\rho(1-\nu^2)/E}/R$ is the ring frequency for a cylindrical bare shell.

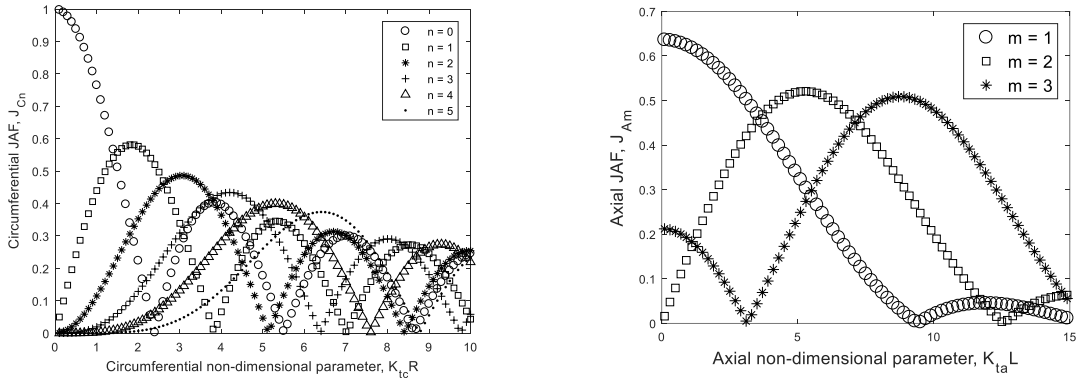

(a) (b)

Figure 4. The circumferential (a) JAFs for lowest order axial modes and (b) JAFs for breathing modes ($n = 0$) against the non-dimensional parameters equal to the Helmholtz number (kR or kL) and k_t is the trace wavenumber in the normal to the shell axis (k_{tc}) or axial (k_{ta}) directions.

Figures 5(a) to 5(d) present the spectra for the displacements predicted at a reference point for each cylinder. The assumptions of blocked pressure is compared with 2-D scattering. Point A depicted in figure 2 is chosen as an example point. Scattering is significant at this position and the point is always located away from stringers and rings. The frequency range is from 200 Hz to 1000 Hz and all the

modes up to 1200 Hz have been included in the calculations. For all the different structures, figure 5(a) to 5(d), three distinct frequency ranges can be observed. Below 300 Hz the response is mostly constant and this is due to the absence of vibration modes. Between 300 and 500 Hz the structures start to show response with peaks corresponding to the first few vibration modes. Above 500 Hz the response increases even further showing a broad peak superimposed by various other peaks.

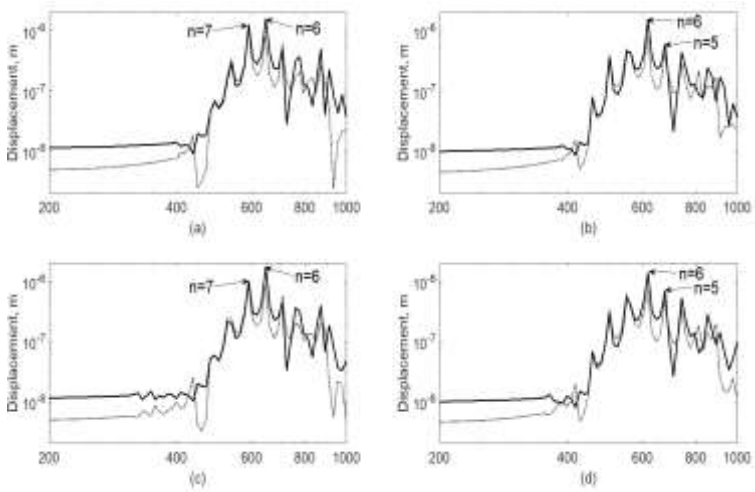

Figure 5. The radial displacement FRF (per unit pressure harmonic excitation) solid lines for blocked pressure results and dotted lines for scattering pressure results in upper figures) at a reference point on the furthermost side of the bare cylinder (a), the stiffened cylinder with 9 rings (b), with 8 stringers (c) and with both rings and stringers (d).

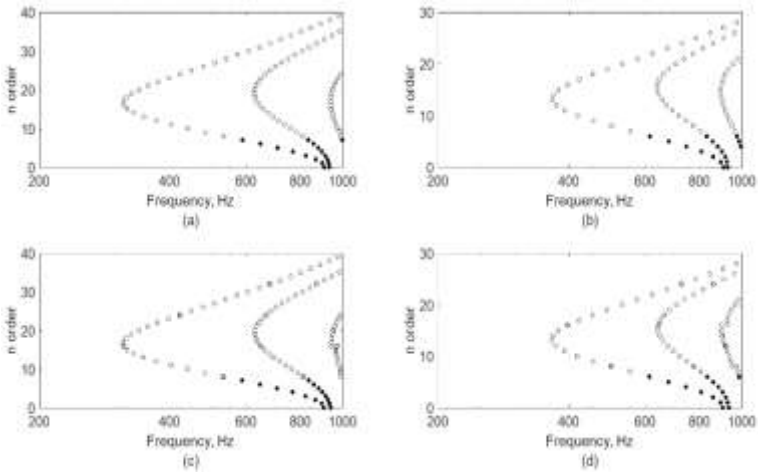

Figure 6. The acoustically excited modes (the predominant modes which corresponds to the peaks in figure 5 are marked by solid circles) at a reference point on the furthermost side for the bare cylinder (a), the stiffened cylinder with 9 rings (b), with 8 stringers (c) and with both rings and stringers (d).

Figures 6(a) to 6(d) show the acoustically excited modes and their frequency response dependency corresponding to the displacement responses in figures 5(a) to 5(d) for each cylinder. The marked solid circles which are the pronounced dominant modes corresponding to the resonant peaks in figure

5. These figures confirm the absence of modes below 300 Hz and show that below 500 Hz the order around the circumference (n) is relatively high. From equation (4) it was found that high order n results in smaller JAF (see figure 4). The response of the structure becomes larger for $n < 8$, which occurs at frequencies above 500 Hz. In this instance and for all the four structures considered, the highest peak in the response correspond to mode $m = 1, n = 6$. Additionally, all the figures show that blocked pressure gives a more conservative prediction of the response compared to the scattering pressure. The difference between the two decreases at the higher frequencies, when the acoustic wavelength is much smaller than the circumferential dimension of the cylinder. For this chosen response point, and for these geometries, the effect of stiffeners is limited.

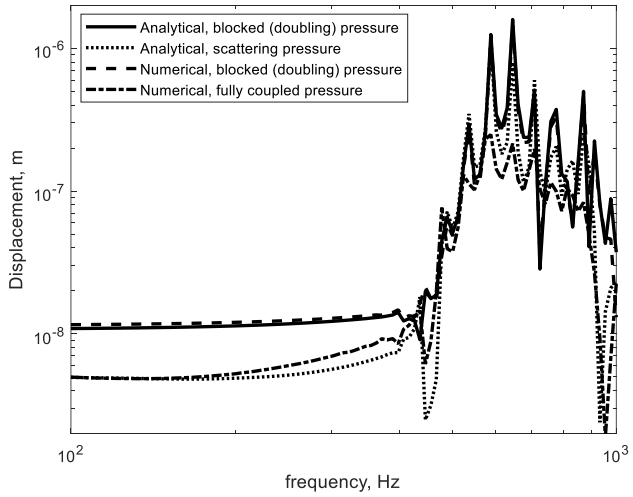

Figure 7. Displacement of the reference point for the bare cylinder: blocked pressure (solid line), 2-D scattered pressure (dotted line), FE blocked pressure (dashed line) and the FE-BE fully coupled pressure (dash - dot line). This shows the effect of the assumed acoustic pressure excitation on the bare cylinder response.

Figure 7 compares analytical predictions with those from a numerical model. This is calculated with both a blocked pressure assumption and with a full FE-BE coupling. Both have been developed in COMSOL and only the case of a bare cylinder has been analysed. The size of structural and acoustic mesh guarantees at least six elements per wavelength in each domain. The prediction based on blocked pressure overlaps completely with that in the FE model and for this reason it is not visible in the figure. In the FE-BE model, two finite cylinders longer than the longest acoustic wavelength in the simulation approximate the semi-infinite rigid cylinders at the ends of the structures. The result shows that in the frequency range away from the pronounced resonances (≤ 400 Hz), the result of the 2-D scattering pressure approximation agrees well with that of the fully coupled analysis, while the prediction of the response based on the blocked pressure approximation is higher. This is because at low frequency the structural vibration is so small that it has negligible re-radiation effect, but the interaction between the sound and the structure geometry is significant in this case. At high frequencies, where resonances occur, the fully coupled model response is lower than the two approximate models. This is likely to be due to radiation damping, the effect of which appears above 400 Hz. The resonant frequencies in the fully coupled response are slightly lower than those in the two approximate models, which is likely to be due to the mass effect of the fluid loading from the surrounded air. The run time for the FE-BE model of the bare cylinder is about 40 hours on a standard desktop computer, while that of the two approximate models is about 5 minutes. For the other stiffened cylinders, the fully coupled FE-BE simulation can be more demanding and has not yet been

addressed by the authors.

5. Conclusions

This paper presented an analytical model to predict the response of cylinders with and without stiffeners due to acoustic plane wave excitation. Results are produced to show the effect of stiffeners on the vibration modes, the modal contribution in the JAFs and acoustic response based on two different incident pressure approximations. The natural frequency grouped behaviour is introduced by the stiffeners, making the cylinder behave like a finite periodic structure. The modes with lower circumference mode order give a larger contribution to the total response. Both of the two approximate pressure assumptions lead to an overestimate of the response. They can significantly reduce the computational time at the cost of sacrificing some accuracy but are still conservative predictions. The analytical model could in the future be improved by including the effect of radiation damping.

Acknowledgments

The authors would like to acknowledge the BISE-FEE Joint Laboratory, who funded the project of acoustic fatigue prediction for advanced aerospace structures.

References

[1] Wijker J 2018 Miles' Equation in Random vibrations: Theory and applications in spacecraft structures design *Solid Mechanics and Its Applications no. 248* (Switzerland: Springer)
[2] Joshi P, Mulani S B and Kapania R K 2015 Multi-objective vibro-acoustic optimization of stiffened panels *AIAA/ASME Structural Dynamics and Material Conference* **2011-1750**
[3] Davis R B and Fulcher C W 2011 Framework for optimizing the vibroacoustic response of component loaded panels *AIAAJ* **53** 265-72
[4] Division E P 1996 Response prediction by deterministic methods *Structural Acoustics Design Manual* (The Netherlands: ESA Publications Division)
[5] Zhao D, Squicciarini G, and Ferguson N S 2019 The acoustic response of stiffened plates *J Physics: Conf Series* **1264** 012041
[6] Egle D M and Sewall J L 1968 An analysis of free vibration of orthogonally stiffened cylindrical shells with stiffeners treated as discrete elements *AIAAJ* **6** 518-26
[7] Kataoka S and Hida T 2016 Evaluation of stress in vibrating cylindrical shells due to acoustic loading based on theory of shells *ASME 2016 Pressure Vessels and Piping Conference* (Canada) p V003T03A019
[8] Cunningham P R, Langley R S and White R G 2003 Dynamic response of doubly curved honeycomb sandwich panels to random acoustic excitation Part 2: Theoretical study *J. Sound Vib.* **264** 605-37
[9] Fahy F J 1994 Acoustically induced vibration of structures *Sound and Structural Vibration: Radiation, Transmission and Response* (London; San Diego; New York: Academic Press) p 221
[10] Coyette J P, Lielens G, Robbe M, and Neple P 2005 An efficient method for evaluating diffuse field joint acceptance functions for cylindrical and truncated conical geometries *J. Acous. Soc. Am.* **117** 1009-19
[11] Seon G and Roy N 2011 Vibro-acoustic response to diffuse acoustic field using a modal approach and application to the IXV re-entry vehicle design justification *EUCASS 2011*
[12] Flügge W and Persen L N 1961 Stresses in shells *J Appl Mech* **28** 477-8
[13] Leissa A W 1973 Thin circular cylindrical shells *Vibration of shells United States: Scientific and Technical Information Office* (National Aeronautics and Space Administration) p 49
[14] Meirovitch L 1967 *Analytical Methods in Vibrations* (New York: Macmillan)
[15] Skudrzyk E 1971 The wave equation in cylindrical coordinates and its applications *The Foundations of Acoustics: Basic Mathematics and Basic Acoustics* (Wien: Springer Vienna) p 446